

# INFERRING DOMAIN-AVERAGED CLOUD PROPERTIES FROM THE ARM OBSERVATIONS AND TESTING THE PCLOS MODELS

Yingtao Ma <sup>a</sup> and Robert G. Ellingson <sup>b</sup>

<sup>a</sup> Department of Meteorology, University of Maryland, College Park, MD 20742  
Email: [ytma@atmos.umd.edu](mailto:ytma@atmos.umd.edu)

<sup>b</sup> Department of Meteorology, Florida State University, Tallahassee, FL 32306  
Email: [bobe@met.fsu.edu](mailto:bobe@met.fsu.edu); Tel: (850) 644-8583

## 1. INTRODUCTION

In climate studies, longwave radiation fluxes and heating rate are usually calculated as the weighted average of clear and overcast values, i.e.,

$$F = (1 - N)F_{\text{clear}} + NF_{\text{overcast}} \quad (1)$$

where,  $F$  is downwelling flux of radiant energy at the surface; subscripts clear and overcast denote fluxes for those conditions.  $N$  is the absolute cloud fraction, usually assumed to be the fractional coverage of the vertical projections of plane-parallel clouds. However, real cloud fields are non-uniform in both morphological and microphysical senses. The error due to neglecting the 3D effects can be climatically significant. (Harshvardhan and Weinman 1982; Ellingson 1982; Heidinger and Cox 1996; Han and Ellingson 1999; Takara and Ellingson 2000)

Three characteristics of 3D clouds have been found to be important for longwave radiative transfer. They are: (1) the 3D geometrical structure of the cloud fields (Geometrical effect), (2) the horizontal variation of cloud optical depth (Variable optical depth effect), and (3) the vertical variation of cloud temperature (Non-isothermal cloud effect). At zenith angles  $\theta > 0$ , vertically extended clouds project greater areas than the PPH clouds. This is denoted as the geometrical effect. By neglecting the geometrical effect the PPH approximation will underestimate the downwelling longwave flux.

One way to incorporate the 3D geometrical effect in climate studies is through the use of an effective cloud fraction (Ellingson 1982; Han and Ellingson 1999). That is,

$$F = (1 - N_e) F_{\text{clear}} + N_e F_{\text{overcast}} \quad (2)$$

The effective cloud fraction,  $N_e$ , is the plane-parallel cloud fraction that generates the same flux as the detailed models for a given broken cloud field after taking into account the effects of geometric shapes, size, spatial distribution and absolute amount ( $N$ ) of clouds. These effects may be integrated into  $N_e$  through a single cloud field property – the Probability of Clear Line Of Sight (PCLOS). The PCLOS also plays an important role in accounting for longwave 3D effects caused by variable cloud optical depth and vertical change of cloud

temperature. In this study we use a variety of data from the Atmospheric Radiation Measurement (ARM; Stokes and Schwartz 1994) program to test several different PCLOS models.

## 2. THE PROBABILITY OF A CLEAR LINE OF SIGHT (PCLOS)

For a given absolute cloud fraction,  $N$ , the PCLOS is a function of cloud shape, aspect ratio and distribution of the clouds in the cloud field. Assuming the clouds have identical base heights, are randomly distributed in an infinitely large horizontal plane, and are right cylinders or semi-ellipsoids, the PCLOS at zenith angle  $\theta$  is given as (Ellingson 1982; Ma 2004)

$$p(\theta) = (1 - N)^{f(\theta)}$$

$$\text{where } f(\theta) = \begin{cases} 1 + \frac{4}{\pi} \beta \tan \theta, & \text{for right - cylindrical clouds.} \\ \frac{1}{2} \left( \sqrt{1 + 4\beta^2 \tan^2 \theta} + 1 \right), & \text{for semi - ellipsoidal clouds.} \end{cases}$$

$\beta$  is the cloud aspect ratio defined as the ratio of the cloud height to the horizontal size. Theoretically, the PCLOS decreases monotonically from  $(1-N)$  at zenith to zero at the horizon.

## 3. ARM CLOUD OBSERVATIONS: FROM TIME SERIES TO DOMAIN AVERAGE

The ARM cloud sensing instruments are fixed at the surface at the ARM Southern Great Plains (SGP) site, and most can only sample the cloud field in the zenith direction. Assuming the statistical properties of the cloud field do not change as the clouds move with the mean wind allows us to infer the domain-averaged properties from a time series of observations. This raises two questions: (1) For a given wind condition, over how long a period or over how many individual clouds does one need to average to obtain representative statistics? and (2) What sampling rate will give the most accurate estimate?

Assuming that the cloud field is a homogeneous and generated by an isotropic random process, the target domain is a rectangular area and the sampling transect is located at the center of the target area, the sampling error

can be estimated from the correlation function of the cloud field, the number of observations and the interval between observations. Using the cloud fraction as an example, the sampling error can be expressed as:

$$\sigma_{\hat{N}}^2 = \sigma_N^2 \left[ \frac{1}{n} + \frac{2}{n^2} \sum_{i=1}^{n-1} (n-i) r(i\Delta l) \right] \quad (4)$$

where  $\hat{N}$  is the estimate of the cloud fraction along the single transect;  $\sigma_{\hat{N}}^2$  denotes the variance of  $\hat{N}$ , which is a function of the number of sample points,  $n$ , and the correlation function of the cloud field,  $r$ ;  $\Delta l$  is the interval between two consecutive observations;  $\sigma_N^2$  is the variance of the cloud field. (Kagan, 1997)

The correlation function in equation (4) describes the statistical spatial structure of the cloud field. Figure 1 shows the estimated correlation functions for 45 days of single layer cumulus cloud fields over the ARM CART site from July 2000 through October 2001. Also shown in the figure is the fitted correlation model, which is assumed to be a negative exponential function. The e-folding parameter for the correlation model,  $\rho_0$  is estimated to be 1267m.

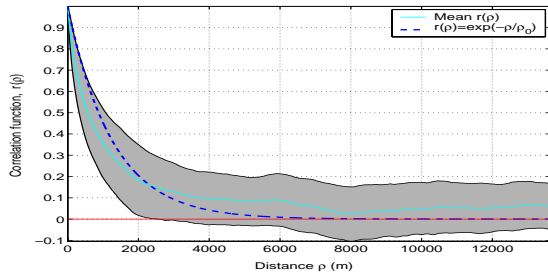


Fig. 1. Observed and modeled correlation functions for single layer cumulus cloud field of the ARM CART site.

Based on an analysis of four cloud resolving model generated cloud fields with (4) and the measured correlation function, we conclude that: (1) For a domain size =  $100\rho_0 \times 100\rho_0$ , a transect of length  $50\rho_0$  can achieve a relative root-mean-square (RRMS) error of about 30% when inferring  $N$  (assuming a 10 m/s wind speed,  $50\rho_0$  corresponds to about 100min); (2) When the sampling interval  $\Delta l < \rho_0$ , further increasing sampling rate does not significantly improve the accuracy; and (3) If  $\Delta l > 3\rho_0$ , the observations can be seen as independent of each other.

#### 4. DETERMINING THE CLOUD FIELD PARMETERS FROM THE ARM CLOUD OBSERVATIONS

##### 4.1 The PCLOS

The PCLOS is estimated from Total Sky Imager (TSI) data by determining the fraction of clear pixels within each  $1^\circ$  annular ring from zenith to instrument horizon for each image on days when only cumulus clouds were present. PCLOS( $\theta$ ) for a given period is determined by averaging over several images. Figure 2 shows  $p(\theta)/(1-N)$  for 86 cumulus cloud fields selected from July 2000 to October 2001. This normalized PCLOS is the conditional probability of a clear line of sight given that the line of sight reaches the cloud base level in the  $(1-N)$  portion of the cloud field. Alternatively,  $1 - p(\theta)/(1-N)$  is the probability of seeing cloud sides at an angle  $\theta$  given that the line of sight reaches the cloud base level in the  $(1-N)$  portion of the cloud field. Generally, the curve decreases from 1 at zenith to 0 at horizon. Note that some cases have a conditional probability larger than 1 at some angles. This is likely caused by the presence of a cloud streak or an inhomogeneity in the cloud field.

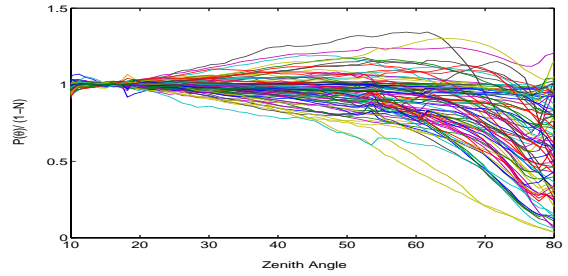


Fig. 2. The PCLOS inferred from the TSI .

##### 4.2 Cloud Thickness

Several laser instruments at the ARM-CART site directly measure cloud base height. The Active Remotely-Sensed Clouds Locations (ARSCL) products give a good estimate of the cloud base height by merging these laser observations. Due to the clutter problem, sometimes, it is difficult to determine the top height of the fair weather cumulus from the cloud radar (MMCR) observations. In this study, we combined the information from the MMCR and the relative humidity (RH) profiles to infer the needed cloud top height. First, an initial cloud top height is obtained from the ARSCL data. This top height is checked with the available RH profiles. If the RH profiles clearly indicate a cloud top layer and this layer is much different from the MMCR measurement, then we take the RH height as the final cloud top height. Figure 3 shows histograms of the obtained cloud thicknesses. The correction based on the RH profiles mainly eliminates some larger cloud thicknesses reported by the MMCR. Figure 4 shows the aspect ratios (thickness / horizontal size) of the single layer cumuli over the ARM SGP site. For most of the fair weather cumulus clouds, the aspect ratio has value less than 1.

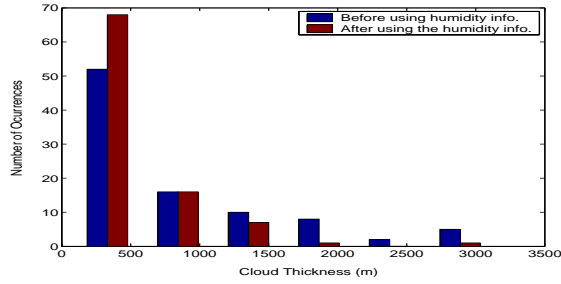


Fig. 3. Histograms of the cloud thickness determined before and after taking into account the relative humidity information, for 93 cases of single layer cumulus fields over the ARM CART site.

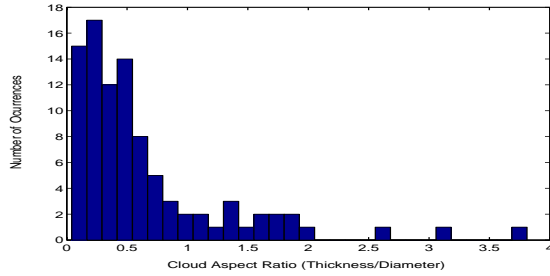


Fig. 4. Histogram of the cloud aspect ratio for the 93 cases.

### 4.3 Cloud Spacing and Horizontal Size

Assuming the cloud field properties do not change significantly as they move past at the mean wind speed, the spacing and horizontal sizes are estimated as the products of the wind speed and the lengths of the time intervals from a time series of observations of the cloud field. The wind speed at cloud height is determined from the 915 MHz Radar Wind Profiler (RWP915) data. The Narrow Field of View Sensor (NFOV) data is used to infer the spacing and cloud time interval lengths. Figure 5 shows the histograms of the cloud sizes and spacing. For most selected cases, the median cloud size and spacing are less than 1000 m and 2000 m, respectively.

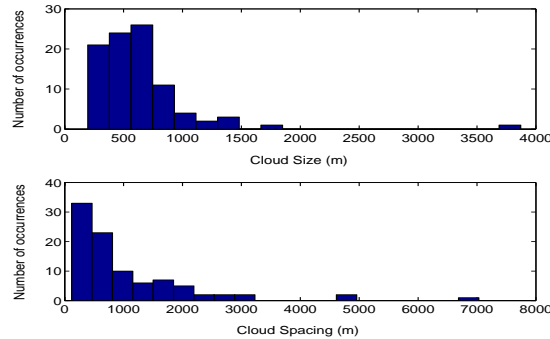


Fig. 5. Histograms of the cloud sizes and spacing for the data used in this study.

### 4.4 Absolute Cloud Fraction

The absolute cloud amount is defined as the fractional coverage of the vertical projections of the

clouds on the surface. We inferred the absolute amount by using the same assumptions as for cloud spacing, and estimated  $N=l/L$ , where  $L$  is the total length of a time series of observation and  $l$  is the length of the cloud segments.

The ARM NFOV, TSI, Whole Sky Imager (WSI) and ARSCL data have been used to obtain  $N$ . When using the TSI and the WSI, the image sequence of the central circle of a field-of-view of  $20^\circ$  is used to calculate  $N$ . Figure 6 gives a comparison of the four  $N$ 's. The  $N_{WSI}$  agree well with the  $N_{TSI}$  but with a little larger variance, while the  $N_{NFOV}$  and the  $N_{ARSCL}$  tend to overestimate the cloud fraction relative to  $N_{TSI}$  or  $N_{WSI}$ . The cause of these biases may be due to the sensitivity of the instruments to the various clouds and the cloud decision algorithms used to infer cloudiness. The TSI and the WSI detect only visible and relatively thick clouds, while the NFOV and the laser instruments are sensitive to thin and sub-visible high clouds.

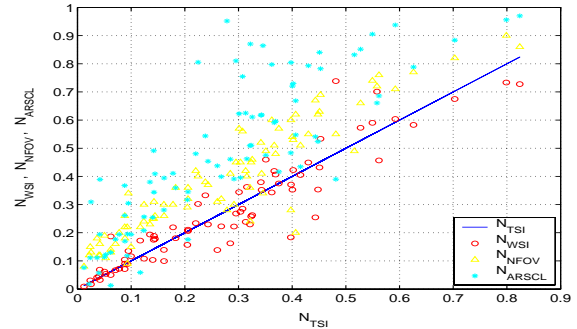


Fig. 6. A comparison of the absolute cloud fraction estimated from the TSI, WSI, NFOV and the ARSCL cloud base data.

## 5. COMARING THE VARIOUS PCLOS MODELS WITH THE TSI OBSERVATIONS

Figure 7 shows the differences between model ( $PCLOS_{model}$ ) and observed  $PCLOS$  ( $PCLOS_{TSI}$ ). All curves in the figures are averages over 38 non-streak cases selected from July 2000 through October 2001 whose cloud thicknesses were confirmed with the relative humidity data. For most models, the average difference between the model  $PCLOS$  and the TSI observations is within  $\pm 0.1$ ; the standard deviation of the differences is less than 0.2. Most models tend to underestimate the  $PCLOS$  in  $30^\circ < \theta < 70^\circ$ , and those models that assume a Poisson cloud distribution give better results. Cloud inclination angel has large impact on the modeling of the  $PCLOS$ , but we do not account for that in this study.

Figure 8 shows the statistics of various model predictions of the cloud side effect and that inferred from the TSI observations. The cloud side effect ( $CSE$ ) is defined as

$$CSE = 2 \int_0^1 [1 - N - P_{clr}(\mu)] u du \quad (5)$$

In the plot, the 16<sup>th</sup> column is the TSI *CSE*, which indicates that for those fair weather cumulus clouds over the ARM CART site, the mean flux departure at the surface due to the cloud side effects is about  $3.7 \pm 2.5$  W/m<sup>2</sup> (assuming the cloud base height is 1.5 km and midlatitude summer conditions). Among the model predictions, we see that the randomly distributed hemispheres generated better results.

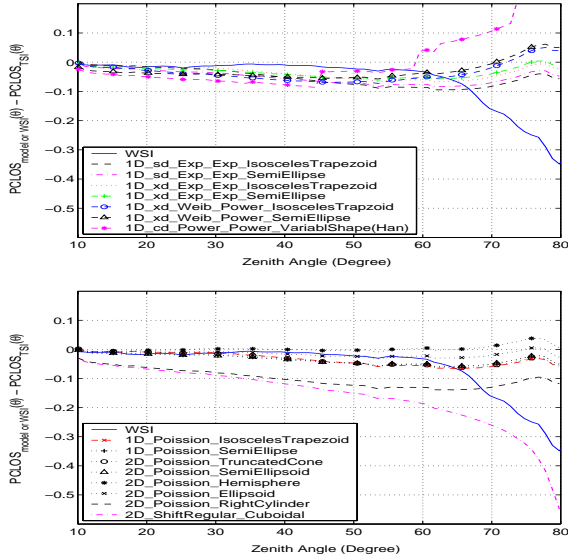


Fig. 7 Average ( $PCLOS_{model} - PCLOS_{TSI}$ ) for 38 cases.

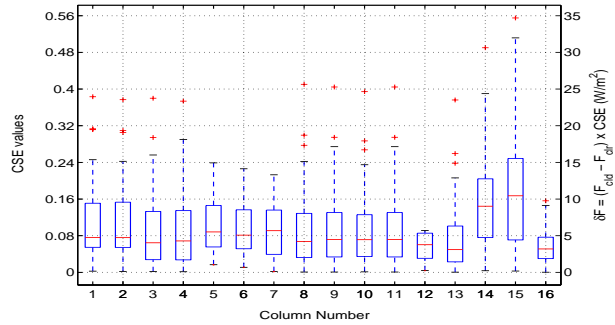


Fig. 8. Statistics of the model predictions of the *CSE* values and those inferred from the TSI observations (column No.16). Column No.12 is the model that assumes the clouds are randomly distributed hemispheres.

## 6. SUMMARY AND CONCLUSIONS

To evaluate a cloud sampling strategy using observations from a fixed point, an evaluation technique was developed and tested with the CRM/LES model data. For a homogeneous random field, the accuracy of the domain-averaged value inferred from a single transect depends on the covariance structure of the field. A field with larger correlation scale needs a longer sampling transect to achieve the desired accuracy. Observations made within the distance of correlation scale contain

redundant information and are not independent of each other. For the clouds sampled in this study, the e-folding parameter for the correlation model is about 1267m.

Compared with the PCLOS inferred from the ARM total sky images, the PCLOS models can roughly capture the shape of PCLOS. Among the models, those assuming a Poisson cloud distribution and round-top cloud shape tend to give better results. However, since the clouds sampled in this study are relatively small, these results should not be expected to hold for all cumulus clouds. We plan to extend the results by looking at more mature, tropical fair-weather cumulus clouds.

## REFERENCES

Ellingson, R. G. 1982: On the effects of cumulus dimensions on longwave irradiance and heating rate calculations. *J. Atmos. Sci.*, **39**, 886-896.

Han, D., and R. G. Ellingson, 1999: Cumulus cloud formulations for longwave radiation calculations. *J. Atmos. Sci.*, **56**, 837-851.

Harshvadhan, 1982 and J. A. Weinman, 1982: Infrared radiative transfer through a regular array of cuboidal clouds. *J. Atmos. Sci.*, **39**, 431-439

Heidinger, A. K., and S. K. Cox, 1996: Finite-cloud effects in longwave radiative transfer. *J. Atmos. Sci.*, **53**, 953-963.

Kagan, R. L, 1997: *Averaging of Meteorological Fields*. Translated from Russian. Ed. by L. S. Gandin and T. M. Smith. Kluwer Academic, 279 pp.

Ma, Y., 2004: Longwave radiation transfer through 3D cloud fields: Testing of the probability of clear line of sight models with the ARM cloud observations. Ph.D. dissertation, University of Maryland at College Park, 174 pp.

Stokes, G. M., and S. E. Schwartz, 1994: The Atmosphere Radiation Measurement (ARM) program: Programmatic background and design of the cloud and radiation test bed. *Bull. Amer. Meteor. Soc.*, **75**, 1201-1221.

Takara, E. E., and R. G. Ellingson, 2000: Broken cloud field longwave-scattering effects. *J. Atmos. Sci.*, **57**, 1298-1310.